Reactions of Spinach Nitrite Reductase with Its Substrate, Nitrite, and a Putative Intermediate, Hydroxylamine†

Sofya Kuznetsova,‡ David B. Knaff,§,|| Masakazu Hirasawa,§ Pierre Sétif,‡ and Tony A. Mattioli*,‡

Service de Bioénergétique and CNRS URA 2096, Département de Biologie Joliot Curie, CEA Saclay, 91191 Gif-sur-Yvette Cedex, France, and Department of Chemistry and Biochemistry and Center for Biotechnology and Genomics, Texas Tech University, Lubbock, Texas 79409-1061

Received June 8, 2004; Revised Manuscript Received June 22, 2004

ABSTRACT: Plant nitrite reductase (NiR) catalyzes the reduction of nitrite (NO_2^-) to ammonia, using reduced ferredoxin as the electron donor. NiR contains a [4Fe-4S] cluster and an Fe-siroheme, which is the nitrite binding site. In the enzyme's as-isolated form ($[4Fe\text{-}4S]^{2+}/Fe^{3+}$), resonance Raman spectroscopy indicated that the siroheme is in the high-spin ferric hexacoordinated state with a weak sixth axial ligand. Kinetic and spectroscopic experiments showed that the reaction of NiR with NO_2^- results in an unexpectedly EPR-silent complex formed in a single step with a rate constant of $0.45 \pm 0.01\ s^{-1}$. This binding rate is slow compared to that expected from the NiR turnover rates reported in the literature, suggesting that binding of NO_2^- to the as-isolated form of NiR is not the predominant type of substrate binding during enzyme turnover. Resonance Raman spectroscopic characterization of this complex indicated that (i) the siroheme iron is low-spin hexacoordinated ferric, (ii) the ligand coordination is unusually heterogeneous, and (iii) the ligand is not nitric oxide, most likely NO_2^-. The reaction of oxidized NiR with hydroxylamine (NH_2OH), a putative intermediate, results in a ferrous siroheme−NO complex that is spectroscopically identical to the one observed during NiR turnover. Resonance Raman and absorption spectroscopy data show that the reaction of oxidized NiR ($[4Fe\text{-}4S]^{2+}/Fe^{3+}$) with hydroxylamine is binding-limited, while the NH_2OH conversion to nitric oxide is much faster.

The assimilatory ferredoxin-dependent nitrite reductases of plants and algae are soluble chloroplast enzymes that catalyze the reduction of nitrite to ammonia in a reaction that involves six electrons and eight protons (*1*). These nitrite reductases (NiR),[1] and the homologous assimilatory nitrite reductases from cyanobacteria, use reduced ferredoxin (Fd) as the physiological electron donor. As ferredoxin is a one-electron donor and the enzyme has been shown to form a 1:1 complex with ferredoxin, the electrons presumably arrive at NiR one at a time (*1*). Nitrite reductase contains two prosthetic groups. One is a siroheme, an Fe isobacteriochlorin that is uniquely present as a prosthetic group in nitrite and sulfite reductases (*2*). The other is a [4Fe-4S] cluster which is coordinated to four cysteine residues, a sulfur atom of one of these cysteines acting as an axial ligand to the siroheme group (*3*, *4*). Both of these prosthetic groups act as independent one-electron carriers in oxidation−reduction titrations, with an E_m value for the siroheme that is approximately 75 mV more positive than that of the [4Fe-4S] cluster (*1*). Siroheme serves as the nitrite-binding site, with the substrate anion binding to the heme iron center via its nitrogen atom (*1*). Electrons from ferredoxin are first transferred to the [4Fe-4S] cluster of nitrite reductase (*5*), then to the siroheme, and finally to the substrate which remains bound until its complete reduction to ammonia (*1*). Sulfite reductase (SiR) from *Escherichia coli*, which catalyzes the six-electron reduction of sulfite to sulfide using NADPH as the electron donor, is a heterodimeric protein with one of the subunits being the siroheme protein (SiR-HP) that has the same prosthetic group content as NiR and which can reduce nitrite as an alternative substrate. Although the three-dimensional structure of plant NiRs remains unknown, a high-resolution structure is available for SiR-HP (*6*, *7*) and, given the similarities of the catalytic sites of the two enzymes, serves as a useful model, at least in the active site region, for the related NiR (*8*).

For NiR as isolated, both the [4Fe-4S] cluster and the siroheme are oxidized ($[4Fe\text{-}4S]^{2+}/Fe^{3+}$) and the siroheme iron is in a ferric high-spin state. Addition of its substrate, NO_2^-, leads to the formation of an unexpectedly EPR-silent

† S.K. has been supported by a Long-Term FEBS fellowship. T.A.M. gratefully acknowledges financial support from the Regional Council of the Ile-de-France for an equipment grant (SESAME). This work was supported, in part, by a grant (to D.B.K.) from the U.S. Department of Energy (DE-FG02-99ER20346).

* To whom correspondence should be addressed. Phone: (+33) 169 08 41 66. Fax: (+33) 169 08 87 17. E-mail: tony.mattioli@cea.fr.

‡ CEA Saclay.

§ Department of Chemistry and Biochemistry, Texas Tech University.

|| Center for Biotechnology and Genomics, Texas Tech University.

[1] Abbreviations: NiR, ferredoxin:nitrite oxidoreductase; SiR, sulfite reductase; SiR-HP, *E. coli* sulfite reductase hemoprotein subunit; NH_2-OH, hydroxylamine; oxyHb, oxyhemoglobin; metHb, methemoglobin; OEP, octaethylporphyrin; OEC, octaethylchlorin; OEiBC, octaethylisobacteriochlorin; DSR, desulforubidin; Fe(III)OEiBC $DMSO_2$, Fe(III)-containing OEiBC in dimethyl sulfoxide; Fe(II)OEiBC 1,2-DiMeIm or Fe(III,II)OEiBC *N*-$MeIm_2$, Fe(III)- or Fe(II)-containing OEiBC complexes with 1,2-dimethylimidazole or *N*-methylimidazole, respectively; Fe(III)OEiBC Cl, Fe(II)-containing OEiBC in chloroform; Fe(II)OEiBC, Fe(II)-containing OEiBC in benzene; fwhm, full width at half-maximum.

10.1021/bi048826r CCC: $27.50
Published on Web 07/30/2004

complex (*9*). SiR-HP also generates an EPR-silent complex upon binding either its physiological substrate, sulfite, or the alternative substrate, nitrite. The optical absorption spectrum of NiR has been found to undergo changes, resulting from nitrite binding, characteristic of the high-spin to low-spin transition for a ferric heme (*10*). A detailed Mössbauer spectroscopic study of SiR-HP, along with magnetization data obtained with both SiR-HP and NiR, showed that the siroheme in the substrate complexes of these enzymes is in the ferric $S = {}^1/_2$ state, allowing elimination of some possible reasons for the EPR-silent nature of these complexes (*11*). An interaction with a neighboring spin and a very high degree of anisotropy of the **g**-tensor have both been found to be unlikely. On the other hand, an excessive heterogeneity in the *g* values of these complexes (*g* strain), resulting in an EPR signal being too broad to be observed, has been suggested to be the most probable cause for the EPR silence (*11*). However, it is still not known whether the siroheme ligand in the EPR-silent complex formed upon reaction of oxidized NiR ($[4Fe\text{-}4S]^{2+}/Fe^{3+}$) with its substrate is indeed nitrite itself or whether the substrate has undergone some modification or partial reduction.

A nitric oxide complex with reduced siroheme ($[4Fe\text{-}4S]^{2+}/Fe^{2+}-NO$), presumably formed by the two-electron reduction of the EPR-silent NiR enzyme−substrate complex, has been characterized by EPR spectroscopy (*3*). This complex (with a characteristic axial EPR signal at $g_x = g_y = 2.06$ and $g_z = 2.007$) is presumed to be an intermediate in nitrite reductase turnover (*3*, *12*). A similar $[4Fe\text{-}4S]^{2+}/Fe^{2+}-NO$ complex has been found to be the most prominent and stable intermediate observed during photoinduced nitrite reduction by *E. coli* sulfite reductase with deazariboflavin as an electron donor (*13*).

Hydroxylamine (NH_2OH), which is two electrons more oxidized than ammonia, has been proposed as an intermediate that might be formed after the formation of nitric oxide, during the reduction of nitrite to ammonia catalyzed by NiR (*1*). Some plant nitrite reductases have been shown to be able to reduce hydroxylamine to ammonia (*14*), and this reaction has also been documented for *E. coli* cytochrome *c* nitrite reductase, an enzyme that also catalyzes a six-electron reduction of nitrite to ammonia (*15*). However, the hydroxylamine complex of NiR, if it is indeed an intermediate formed during enzyme turnover, has never actually been detected and may be EPR-silent. It is possible that the intermediate in the enzyme turnover is the $[4Fe\text{-}4S]^{2+}/Fe^{3+}-NH_2OH$ state, as has been suggested for cytochrome *c* nitrite reductase (*16*, *17*). An attempt to form this intermediate by incubation of oxidized NiR with excess hydroxylamine results in the slow formation of a stable complex (*10*) that, in terms of its absorption and EPR spectra, is identical to the $[4Fe\text{-}4S]^{2+}/Fe^{2+}-NO$ complex described above (*4*, *18*). Little is known about the mechanism of this reaction.

In the work presented here, we have studied the kinetics of the reaction of oxidized NiR ($[4Fe\text{-}4S]^{2+}/Fe^{3+}$) with nitrite and hydroxylamine and we have characterized the intermediate complexes resulting from these reactions by resonance Raman spectroscopy. Resonance Raman spectroscopy has proved to be a useful tool in the study of hemes and heme-containing enzymes. The frequencies of several core size-related vibrational modes of the heme groups are sensitive to the oxidation state and the spin state of the central Fe atom as well as to the nature of the axial ligands. Although the vibrational spectra of the siroheme group of NiR and SiR, due to their lower 2-fold symmetry, are more complex and thus more difficult to interpret than those of more highly 4-fold symmetric porphyrins, significant progress in their study has been made. Several siroheme-containing enzymes have been studied by resonance Raman spectroscopy. The Soret-excited resonance Raman spectra of siroheme in three sulfite reductases, one dissimilatory [desulforubidin (DSR) from *Desulfovibrio baculatus* (*19*)] and two assimilatory ones [low-molecular weight sulfite reductase from *Desulfovibrio vulgaris* (*19*) and *E. coli* sulfite reductase (*20*)], have been reported. For the latter protein, the complexes of the reduced enzyme with NO, CO, and cyanide have been characterized (*20*) and these ligand modes have been identified (*21*). Spinach NiR has also been studied by resonance Raman spectroscopy by Ondrias *et al.* (*22*), although the reaction of oxidized NiR ($[4Fe\text{-}4S]^{2+}/Fe^{3+}$) with nitrite and hydroxylamine was not examined in this earlier work because of high levels of background fluorescence in the resulting complexes. Resonance Raman spectra and band assignments have also been reported for siroheme (*20*) and the siroheme model compound nickel(II) octaethylisobacteriochlorin (OEiBC) (*23*). The assignment of individual bands was substantiated by a comparison to the normal modes calculated for the model Ni OEiBC (*23*).

EXPERIMENTAL PROCEDURES

Materials

Spinach nitrite reductase (EC 1.7.7.1) was prepared using the procedure of Hirasawa *et al.* (*24*). The UV−visible absorption spectrum of the purified enzyme exhibits maxima at 278, 390, and 573 nm, as previously reported (*10*, *25*). A molar extinction coefficient ϵ of 40 000 M^{-1} cm^{-1} at 390 nm (*26*) was used to measure the enzyme concentration. The concentration of the enzyme stock solution used for low-temperature resonance Raman measurements was 1.56 mM, and 195 μM for measurements carried out at room temperature. The buffer for both stock solutions was 50 mM potassium phosphate (pH 7.8). When necessary, the stock solutions were diluted to the desired final concentration with 20 mM Tricine (pH 7.8). Tricine and KH_2PO_4 were purchased from Sigma. NH_2OH hydrochloride (Sigma), KCN (Sigma), and 99.99% $NaNO_2$ (Aldrich) were used without further purification. NO gas was obtained from Messer.

Nitrite Reductase Complexes

NiR $[4Fe\text{-}4S]^{2+}/Fe^{3+}-CN^-$. The nitrite reductase complex with cyanide was prepared by incubation of 167 μM NiR with a 21 mM KCN solution in 20 mM Tricine (pH 7.8) for 50 min. The EPR spectrum of the sample shows full conversion of the high-spin Fe^{3+} siroheme signal, characteristic of the free oxidized enzyme, into a low-spin one, indicative of CN^- complex formation (*27*).

NiR $[4Fe\text{-}4S]^{2+}/Fe^{2+}-NO$. The complex of reduced NiR with nitric oxide was formed by incubation of 167 μM oxidized NiR with excess hydroxylamine (71 mM). This reaction has been shown to lead to formation of the Fe^{2+} siroheme−NO complex [see the introductory section (*4*, *18*)]. Our previous EPR measurements (*18*) have shown that the

addition of 10 mM NH_2OH results in full conversion of 10 μM NiR into the $[4Fe\text{-}4S]^{2+}/Fe^{2+}-NO$ state within 40 min. The $g \sim 2$ EPR signal of this $[4Fe\text{-}4S]^{2+}/Fe^{2+}-NO$ complex is an indication of an $S = {}^1/_2$ $\{FeNO\}^7$ unit (Enemark−Feltham notation) which is best rationalized as involving a low-spin Fe^{2+} ($S = 0$; six d electrons) and $NO^{\bullet}$ ($S = {}^1/_2$, one π^* electron).

NiR [4Fe-4S]$^{2+}$/Fe^{3+}−NO. The nitric oxide complex of oxidized NiR was prepared by adding 250 μM NO to 98 μM $[4Fe\text{-}4S]^{2+}/Fe^{3+}$ NiR, using an aqueous NO solution ([NO] = 500 μM) in distilled water which had been degassed by several cycles of evacuation and argon pumping. The NO concentration of the NO-saturated water solution was estimated using an oxyhemoglobin assay in which absorption changes at 401 nm were measured, using a $\Delta\epsilon_{401(metHb-oxyHb)}$ of 44 ± 5 mM^{-1} cm^{-1} for the NO-induced oxyhemoglobin-to-methemoglobin transition (*28*). The EPR spectrum of a similarly prepared sample showed none of the high-spin siroheme signal characteristic of free oxidized NiR, but only a signal (with $g = 4.04$, 4.04, and 2.0) that can be attributed to the $S = {}^3/_2$ complex of nitric oxide with free ferrous iron (*29*). The absence of any EPR signal that can be attributed to oxidized, high-spin siroheme was taken as a sign of complete $[4Fe\text{-}4S]^{2+}/Fe^{3+}-NO$ complex formation. This EPR-silent NiR $[4Fe\text{-}4S]^{2+}/Fe^{3+}-NO$ complex with the $\{FeNO\}^6$ unit has never been characterized, and can be EPR-silent, as has been demonstrated for the case for the heme $Fe^{3+}-NO$ complex in NO synthase (*30*).

Resonance Raman Spectroscopy

Resonance Raman spectra were recorded using a modified Jobin-Yvon T 64000 single-stage monochromator equipped with a liquid nitrogen-cooled back-thinned charge-coupled device detector. Excitation at 406.7 nm, or in some cases 413.1 nm, was provided by a Spectra Physics (Series 2000) Kr^+ laser. Additional excitations at 363.8 and 441.6 nm were provided by an Ar^+ laser (Coherent, Innova 90) and a He−Cd (Kimmon) laser, respectively. The laser power was less than 10 mW at the sample. A holographic notch filter (Kaiser Optical) was used at the entrance slits (100 μm) to reject stray laser light. Protein samples (ca. 150 μM) were used, and spectra were recorded either at room temperature in a spinning cell or at 15 K using a cold helium gas circulating optical cryostat (STVP-100, Janis Research). Spectra were calibrated using the laser excitation line along with the SO_4^{2-} and ice (15 K experiments) Raman bands from a saturated solution of sodium sulfate. The spectral resolution was better than 3 cm^{-1}. Baseline corrections were performed using GRAMS 32 (Galactic Industries).

Stopped-Flow and Absorption Spectroscopy

Stopped-flow UV−visible absorption measurements were recorded using a Bio-Logic SFM-300 rapid mixing module, a MPS-52 microprocessor unit, and a J&M Tidas 1024 channel diode-array spectrometer. The observation cuvette (0.5 cm path length) had a volume of 47.5 μL, and the apparatus had a dead time of ~2 ms. The entire mixing and observation chamber was held at 10 °C using a Julabo F30 C cryostat circulation bath connected directly to the mixing module. The protein concentration was 75 μM, and the concentration of the $NaNO_2$ stock solution, in 20 mM Tricine buffer (pH 7.8), was 25 mM. NiR (100 μL) was mixed with 100 μL of the stock nitrite solution to initiate the complex formation reaction, which was then followed for 15 s, over the entire spectral region from 250 to 850 nm. The UV−visible spectra of $[4Fe\text{-}4S]^{2+}/Fe^{3+}$ NiR during its reaction with hydroxylamine were recorded at room temperature using the same apparatus with a sampling time of 1 s.

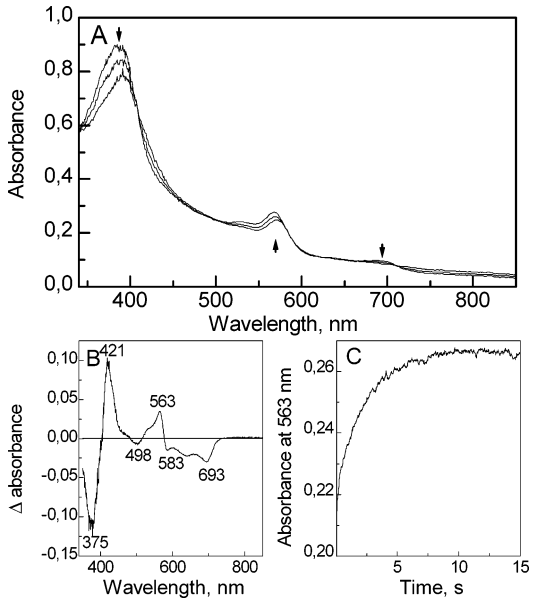

FIGURE 1: Stopped-flow study of the reaction of nitrite reductase with nitrite. (A) Sequential visible absorption spectra of rapidly mixed solutions of 76 μM $[4Fe\text{-}4S]^{2+}/Fe^{3+}$ NiR and 25 mM $NaNO_2$ in 20 mM Tricine (pH 7.8) 0.06, 2, and 9 s after mixing. (B) Absorption difference spectrum of the same sample, 15 s minus 60 ms after mixing. (C) Absorption kinetic trace at 563 nm. The sampling time was 20 ms.

RESULTS AND DISCUSSION

Kinetics of the Oxidized NiR ([4Fe-4S]$^{2+}$/Fe^{3+}) Reaction with Nitrite. Vega and Kamin (*10*) have demonstrated that nitrite binds stoichiometrically to oxidized $[4Fe\text{-}4S]^{2+}/Fe^{3+}$ NiR ($K_d \approx 3$ μM). Similar absorption difference spectra for fully oxidized NiR ($[4Fe\text{-}4S]^{2+}/Fe^{3+}$) complexed with nitrite and without nitrite have been reported by Vega and Kamin (*10*), Hirasawa *et al.* (*31*), Mikami and Ida (*32*), and Bellissimo and Privalle (*26*). Cammack *et al.* (*12*) have found that complete disappearance of the EPR signals characteristic of free oxidized $[4Fe\text{-}4S]^{2+}/Fe^{3+}$ NiR after addition of nitrite to this form of the enzyme took several minutes at 0 °C. However, the kinetics of nitrite binding have not been investigated in detail in any of these earlier studies.

Figure 1 shows the evolution of the absorption spectrum (Figure 1A), the final difference spectrum (Figure 1B), and the kinetics for the reaction of $[4Fe\text{-}4S]^{2+}/Fe^{3+}$ NiR with nitrite (Figure 1C). Nitrite addition results in characteristic spectral shifts in the 390 nm (Soret band) and 580 nm bands, as well as the disappearance of the weak band at 690 nm, as has been previously shown (*10*, *26*, *31*, *32*). The difference spectrum in Figure 1B is in good agreement with those previously reported (*10*, *26*, *31*, *32*). No apparent intermediate species were found in this reaction, and the spectra show a single set of well-defined isosbestic points (Figure 1A).

The kinetic traces of the absorption changes at 563 nm (Figure 1C), as well as those at 421 and 693 nm (not shown),

are the same and indicate that the reaction of $[4Fe\text{-}4S]^{2+}/Fe^{3+}$ NiR with nitrite is complete within 10 s, with apparent first-order kinetics. The apparent rate constant of complex formation calculated from Figure 1C is 0.45 ± 0.01 s^{-1}. It should be pointed out that this binding rate, although compatible with the above observations of Cammack *et al.* (*12*), is rather slow compared to that which might be expected for the substrate binding during catalysis. The turnover rates of NiR reported in the literature vary significantly. Vega and Kamin (*10*) have found a turnover number of 33.3 min^{-1} for NiR with the nonphysiological electron donor sodium dithionite. This turnover rate is compatible with the binding rate reported above. However, this binding rate is much too slow for the V_{max} for Fd-linked activity of spinach NiR of $(12.7 \pm 0.3) \times 10^3$ min^{-1} found by Mikami and Ida (*32*) or an even larger value of 43.8×10^3 min^{-1} (263 000 e^{-1} min^{-1} $heme^{-1}$) reported by Krueger and Siegel (*33*). This discrepancy seems to suggest that binding of NO_2^- to the as-isolated form of nitrite reductase ($[4Fe\text{-}4S]^{2+}/Fe^{3+}$) is not the predominant type of substrate binding during enzyme turnover.

We repeated the stopped-flow experiment with NiR in a non-phosphate-containing buffer, i.e., 30 mM Tris (pH 8.0) containing 150 mM NaCl. The high salt concentration was used for stabilizing the enzyme. The ionic strength of this buffer is similar to that of the phosphate buffer. Mixing with nitrite gave initial and final absorption spectra (and hence difference spectra) very similar to those obtained with the phosphate buffer. However, the kinetics of nitrite binding were even slower ($k \approx 0.1$ s^{-1}) than those observed in the presence of phosphate ($k \approx 0.45$ s^{-1}). Therefore, phosphate clearly does not specifically slow the rate of nitrite binding. To check that the enzyme sample used for these measurements was catalytically active and to assess the apparent discrepancy between the slow binding of nitrite and the fast turnover rates reported in the literature, we performed the following flash-absorption spectroscopy experiment. Ferredoxin reduced by photoexcited photosystem I was used as a reductant under conditions where NiR was present in catalytic amounts in the presence of nitrite, in Tris buffer at 35 mM NaCl. The reoxidation of 3 μM photoreduced ferredoxin due to reduction of NiR was essentially monoexponential with an initial rate of 160 e^{-1} s^{-1} $heme^{-1}$ (approximately 10 000 e^{-1} min^{-1} $heme^{-1}$). The observed rate is not the maximal turnover rate as it is limited by the ferredoxin concentration, and full ferredoxin reoxidation corresponded to up to four full NiR catalytic cycles. This rate is much faster than the rate of nitrite binding observed in stopped-flow experiments. This shows that a critical factor for rapid nitrite binding must be reduction of the enzyme, as previously suggested by Cammack *et al.* (*12*). These authors suggested that it was likely that the mechanism of NiR involved a single one-electron reduction to the $[4Fe\text{-}4S]^{2+}/Fe^{2+}$ form prior to nitrite binding.

The related enzyme, *E. coli* SiR-HP, may serve as a useful model for nitrite binding by NiR. The binding of sulfite to oxidized SiR-HP ($[4Fe\text{-}4S]^{2+}/Fe^{3+}$), which also results in an EPR-silent enzyme−substrate complex, is extremely slow ($t_{1/2} \approx 8.5$ h), while the binding of SO_3^- to fully reduced SiR-HP ($[4Fe\text{-}4S]^{+}/Fe^{2+}$) is complete in 0.2 s (*14*). The model for the enzyme catalytic cycle, proposed by Crane *et al.* (*7*), suggests that the enzyme must be reduced twice before it binds the substrate and the complex of the oxidized enzyme ($[4Fe\text{-}4S]^{2+}/Fe^{3+}$) with SO_3^- does not take part in the catalysis. The extremely slow binding of SO_3^- to the oxidized ($[4Fe\text{-}4S]^{2+}/Fe^{3+}$) SiR-HP is thought to be limited by displacement of phosphate from the binding site (*6*), while enzyme reduction causes phosphate release (even in the absence of substrate) and decreases its affinity for phosphate (*34*). Our resonance Raman data (see below) support the presence of a weak ligand to the siroheme in the NiR as-isolated form ($[4Fe\text{-}4S]^{2+}/Fe^{3+}$), which we suppose to be phosphate from the buffer, as is the case for SiR-HP. This ligand is replaced with nitrite during the formation of the NiR $[4Fe\text{-}4S]^{2+}/Fe^{3+}-NO_2^-$ complex. However, our stopped-flow experiments show that, in the absence of phosphate and with 150 mM NaCl, binding of nitrite to the oxidized enzyme ($[4Fe\text{-}4S]^{2+}/Fe^{3+}$) is even slower. As chloride is not expected to bind more strongly than phosphate, our data suggest that ligand release is not the critical limiting kinetic factor in the case of NiR, but that substrate binding, per se, has a rate that is highly dependent on the reduction state of NiR. It is not yet clear if siroheme reduction is sufficient to produce rapid nitrite binding or whether reduction of both the siroheme and the [4Fe-4S] cluster is necessary for this effect to occur. An alternative explanation, which cannot be excluded from the available data, is that during the NiR turnover, product (NH_4^+) release is coupled to entry of the substrate into the catalytic site.

Resonance Raman Characterization of the NiR Complex with Nitrite. The frequencies of several specific resonance Raman modes observed for metalloporphyrins correlate in an inverse relationship with macrocycle core size, and serve as excellent marker bands for the redox, spin, and coordination state of the central metal atom. For the less symmetric metalloisobacteriochlorins, which have general 2-fold symmetry instead of full 4-fold symmetry of porphyrins, the corresponding core size sensitive band correlations are less straightforward because of the difficulty in reliably assigning these bands. It has been suggested that, unlike the case for other metalloporphyrins, there is no entirely reliable redox state marker for the central Fe atom in the Raman spectra of the siroheme of NiR and SiR (*20*, *23*). For metalloporphyrins with 4-fold symmetry and an unbroken π-electron-conjugated system, the redox state marker is customarily the ν_4 mode, which shifts down from ca. 1370 to ca. 1360 cm^{-1} upon reduction of Fe(III) to Fe(II) (*35*, *36*). However, for siroheme, the corresponding resonance Raman band is weaker and does not exhibit a shift to a lower frequency upon reduction of the siroheme from the Fe^{3+} state to the Fe^{2+} state (*20*, *23*).

On the other hand, it has been proposed that the high-frequency siroheme modes ν_{37} and ν_{10} can serve as Fe spin state markers for siroheme and should also be somewhat sensitive to the Fe coordination state (*20*, *23*). The frequencies of the ν_{10} and ν_{37} bands in FeOEiBC, and in siroheme and siroheme-containing enzymes where the heme is in high-spin six-coordinate, high-spin five-coordinate, and low-spin six-coordinate states, which have been reported in the literature (*19*, *20*, *23*), and the frequencies of these bands observed in this study of several NiR complexes are shown in Figure 2. This figure shows the correlation between the ν_{37} and ν_{10} vibrational frequencies. It can be seen that for

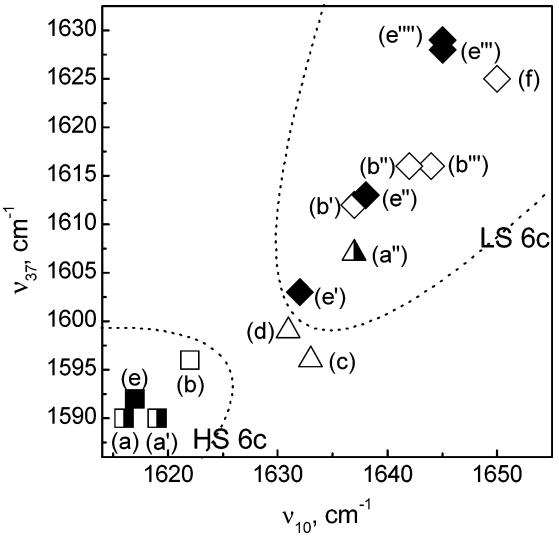

FIGURE 2: Correlation of the observed frequencies of ν_{37} and ν_{10} modes in FeOEiBC, siroheme, and siroheme-containing enzymes. The frequencies of the ν_{37} and ν_{10} modes for high-spin six-coordinate (squares), high-spin five-coordinate (triangles), and low-spin six-coordinate (diamonds) are taken from refs *4*, *5*, and *7* and the work presented here. Half-filled symbols correspond to Fe-OEiBC species, empty symbols to siroheme and siroheme-containing enzymes, and filled symbols to NiR complexes: (a) Fe^{2+} OEiBC 1,2-DiMeIm, (a′) Fe^{3+} OEiBC $DMSO_2$, (a″) Fe^{2+} OEiBC Cl, (b) *E. coli* SiR-HP $[4Fe\text{-}4S]^{2+}/Fe^{3+}$, (b′) SiR-HP $[4Fe\text{-}4S]^{+}/Fe^{2+}-CN^{-}$, (b″) SiR-HP $[4Fe\text{-}4S]^{2+}/Fe^{2+}-CO$, (b‴) SiR-HP $[4Fe\text{-}4S]^{2+}/Fe^{2+}-NO$, (c) DSR, (d) siroheme, (e) NiR $[4Fe\text{-}4S]^{2+}/Fe^{3+}$, (e′) NiR $[4Fe\text{-}4S]^{2+}/Fe^{3+}-CN^{-}$, (e″) NiR $[4Fe\text{-}4S]^{2+}/Fe^{2+}-NO$, (e‴) NiR $[4Fe\text{-}4S]^{2+}/Fe^{3+}-NO$, (e⁗) NiR $[4Fe\text{-}4S]^{2+}/Fe^{3+}-NO_2^{-}$, and (f) low-molecular weight SiR $[4Fe\text{-}4S]^{2+}/Fe^{3+}$ from *D. vulgaris*.

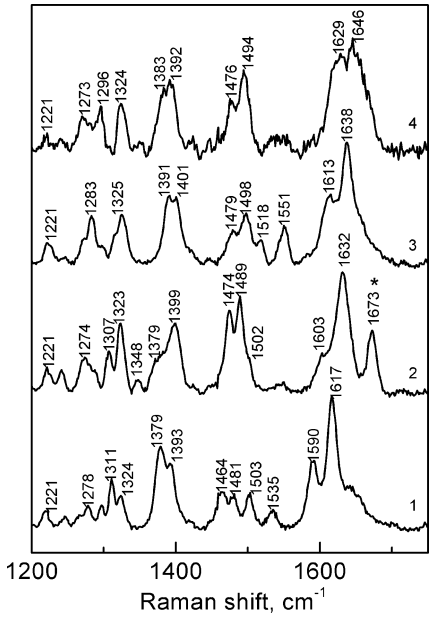

FIGURE 3: Room-temperature resonance Raman spectra of various complexes of NiR obtained with Soret excitation (406.7 nm): (1) 195 μM free oxidized $[4Fe\text{-}4S]^{2+}/Fe^{3+}$ NiR, (2) NiR $[4Fe\text{-}4S]^{2+}/Fe^{3+}-CN^{-}$, 167 μM $[4Fe\text{-}4S]^{2+}/Fe^{3+}$ NiR, and 21 mM KCN, incubated for 50 min at room temperature, (3) NiR $[4Fe\text{-}4S]^{2+}/Fe^{2+}-NO$, formed by incubation of 167 μM $[4Fe\text{-}4S]^{2+}/Fe^{3+}$ NiR with 71 mM hydroxylamine for 50 min at room temperature, and (4) NiR $[4Fe\text{-}4S]^{2+}/Fe^{3+}-NO_2^{-}$ EPR-silent complex, resulting from incubation of 189 μM $[4Fe\text{-}4S]^{2+}/Fe^{3+}$ NiR with 14 mM $NaNO_2^{-}$ for 5 min at room temperature. The exposure time was 30 s for a single spectrum. The presented curves are averages of 240 ($[4Fe\text{-}4S]^{2+}/Fe^{3+}$ NiR), 400 (NiR $[4Fe\text{-}4S]^{2+}/Fe^{3+}-CN^{-}$ and NiR $[4Fe\text{-}4S]^{2+}/Fe^{2+-1}-NO$), and 640 (NiR $[4Fe\text{-}4S]^{2+}/Fe^{3+}-NO_2^{-}$) spectra. The resolution was better than 5 cm^{-1}. An asterisk denotes a spectral band which was observed in room-temperature but not in low-temperature spectra of the cyanide complex. A similar band was observed but not discussed in ref *22*.

six-coordinate Fe^{3+} high-spin siroheme complexes, the ν_{37} and ν_{10} vibrational frequencies are expected to be observed at ca. 1590−1600 and ca. 1615−1625 cm^{-1}, respectively. These same siroheme modes shift to higher frequencies by as much as 10 cm^{-1} when the central iron changes to a low-spin state or five-coordinate state. The correlation shown in Figure 2 also indicates the existence of two more or less well-defined regions for high-spin and low-spin six-coordinate siroheme complexes, which aids in determining the spin state of the siroheme iron from the corresponding resonance Raman spectrum.

To arrive at reliable interpretations for the vibrational spectrum of the EPR-silent complex resulting from the reaction of NiR with nitrite, we have first analyzed the resonance Raman spectra of several complexes of NiR in which the siroheme iron is six-coordinate and in various redox and spin states, as confirmed by EPR spectroscopy (see Experimental Procedures). The resonance Raman spectra of these complexes, compared to that of oxidized resting $[4Fe\text{-}4S]^{2+}/Fe^{3+}$ NiR, are presented in Figure 3.

A comparison of the positions of ν_{10} and ν_{37} bands in oxidized $[4Fe\text{-}4S]^{2+}/Fe^{3+}$ *E. coli* SiR-HP to those in siroheme chloride and model chlorins (OEiBC chloride, OEP, OEC), where the heme is in a five-coordinate ferric high-spin state, and to those in *D. baculatus* DSR, where EPR and Mössbauer studies also show that the siroheme is in the five-coordinate, high-spin ferric state, reveals that in the *E. coli* SiR-HP their frequencies (1622 cm^{-1} for ν_{10} and 1596 cm^{-1} for ν_{37}) are lower by at least 10 cm^{-1} (*20*). On the other hand, for Fe^{3+} OEiBC $(DMSO)_2$, where the heme is in a six-coordinate ferric high-spin state, the frequencies are very similar to those of $[4Fe\text{-}4S]^{2+}/Fe^{3+}$ SiR-HP (*23*). It seems likely that the siroheme in the oxidized $[4Fe\text{-}4S]^{2+}/Fe^{3+}$ SiR-HP has a weak sixth ligand that is not strong enough to change the spin state of the heme. Judging from the SiR-HP X-ray crystal structure, reported in refs *6* and *34*, this ligand is a phosphate ion. The two highest-frequency bands in the siroheme resonance Raman spectrum of free oxidized $[4Fe\text{-}4S]^{2+}/Fe^{3+}$ NiR (Figure 3) are observed at 1617 and 1590 cm^{-1}. We attribute these bands, which agree very well with those observed elsewhere for NiR (*22*) and SiR (*20*, *23*), to the ν_{10} and ν_{37} modes (*22*). These observed frequencies indicate that the siroheme is in an Fe^{3+} high-spin, six-coordinate state (see Figure 2). The sixth ligand could be either a weakly bound water molecule or, most likely, a phosphate ion from the buffer (see Experimental Procedures). In SiR-HP, the phosphate anion bound to the siroheme has been shown to interact with the positively charged amino acids located around the active site that coordinate the physiological substrate, sulfite (*6*, *34*). Three of the four basic amino acids thought to participate in the substrate binding in *E. coli* SiR-HP (Arg 83, Arg 153, and Lys 215) (*6*) are conserved in the spinach NiR sequence, reported by Back *et al*. (*37*) (Arg 41, Arg 111, and Lys 156, respectively) (*8*). If, as is likely, their role is the same as in SiR-HP, they should favor binding of phosphate to oxidized $[4Fe\text{-}4S]^{2+}/Fe^{3+}$ NiR.

The iron atom of the siroheme group in all the NiR complexes shown in Figure 3 is expected to be six-coordinate. The redox and spin states of these were unambiguously confirmed by EPR spectroscopy (see Experimental Procedures). Thus, we can evaluate whether the ν_{10} and ν_{37} bands reflect the spin state of the central iron atom accurately, as predicted from the data in Figure 2. For the resting [4Fe-4S]$^{2+}$/Fe^{3+} NiR protein, the central iron atom is known to be in the Fe^{3+} high-spin state. The resonance Raman spectrum of [4Fe-4S]$^{2+}$/Fe^{3+} NiR exhibits 1590 and 1617 cm^{-1} bands that can be attributed to the ν_{37} and ν_{10} modes, respectively, and as discussed above, their observed frequencies clearly indicate an Fe^{3+} high-spin six-coordinate state for the siroheme. In addition, [4Fe-4S]$^{2+}$/Fe^{3+} NiR exhibits a 1464 cm^{-1} band, which can be attributed to the spin state-sensitive ν_{28} mode (*20*). The spectrum also exhibits a band at 1379 cm^{-1}, corresponding to the ν_4 mode (*22*), which is usually a very good redox state marker in higher-symmetry porphyrins.

The cyano complex of [4Fe-4S]$^{2+}$/Fe^{3+} NiR ([4Fe-4S]$^{2+}$/Fe^{3+}−CN$^-$) has the central iron atom in an Fe^{3+} low-spin state (as confirmed by EPR spectroscopy; see Experimental Procedures). Comparing the resonance Raman spectrum of this complex with that of the resting [4Fe-4S]$^{2+}$/Fe^{3+} NiR protein, we note that there are significant shifts of both the ν_{37} and ν_{10} modes to higher frequencies (+11 and +15 cm^{-1}, respectively) to 1603 and 1632 cm^{-1}, respectively, as expected for these siroheme modes if the heme is converted from a high-spin state to a low-spin state (see Figure 2). There is also a +10 cm^{-1} shift of the 1464 cm^{-1} band to 1474 cm^{-1} for the ν_{28} mode. The band corresponding to the ν_4 mode (1379 cm^{-1}) is in the same position as in [4Fe-4S]$^{2+}$/Fe^{3+} NiR and so seemingly does not shift with spin state conversion.

The resonance Raman spectrum of the NO complex of reduced [4Fe-4S]$^{2+}$/Fe^{2+} NiR ([4Fe-4S]$^{2+}$/Fe^{2+}−NO), a complex in which the siroheme iron atom is in the Fe^{2+}, six-coordinate, low-spin state, exhibits ν_{28}, ν_{37}, and ν_{10} modes (at 1479, 1613, and 1638 cm^{-1}, respectively) that are even higher in frequency than those in the oxidized [4Fe-4S]$^{2+}$/Fe^{3+}−CN$^-$ complex. Interestingly, the ν_4 mode has shifted up in frequency by 12 cm^{-1}, from 1379 to 1391 cm^{-1}. As previously mentioned, the ν_4 mode is a reliable oxidation state marker for higher-symmetry porphyrins and heme groups, where it shifts to lower frequencies (i.e., from ca. 1375 to ca. 1365 cm^{-1}) upon reduction of the central iron atom from Fe^{3+} to Fe^{2+} (*35*, *36*). In the case of the siroheme group of NiR measured in this study, the opposite trend is observed. The ν_4 frequency observed for oxidized and reduced isobacteriochlorins varies significantly depending on their chemical nature, which led Melamed *et al.* (*23*) to conclude that for sirohemes ν_4 is not a very reliable oxidation state marker. However, when one compares the same isobacteriochlorin or isobacteriochlorin-containing protein, ν_4 does shift to higher frequencies by 8−15 cm^{-1} upon reduction (Table 1). Thus, on the basis of the data presented in Table 1 and our analysis, it would seem that the 1379/1391 cm^{-1} band can be used as a reliable oxidation state marker in this study of the siroheme group of NiR, though it exhibits a shifting trend that is the opposite of that seen for higher 4-fold symmetry hemes and porphyrins.

Table 1: Observed Frequencies for the ν_4 Band in Oxidized and Reduced Isobacteriochlorins

heme or protein complex	Fe^{3+}, ν_4 (cm^{-1})	Fe^{2+}, ν_4 (cm^{-1})	ref
DSR	1365	1380	*19*
Fe^{3+} OEiBC $DMSO_2$	1374		*23*
Fe^{2+} OEiBC 1,2-DiMeIm		1383	*23*
Fe$^{3+/2+}$ OEiBC *N*-$MeIm_2$	1380	1388	*23*
Fe^{3+} OEiBC Cl	1373		*23*
Fe^{2+} OEiBC		1385	*23*
SiR-HP [4Fe-4S]$^{2+}$/Fe^{3+}	1375	1383	*20*
SiR-HP [4Fe-4S]$^{2+}$/Fe^{2+}−NO		1384	*20*
SiR-HP [4Fe-4S]$^{2+}$/Fe^{2+}−CN$^-$		1386	*20*
SiR-HP [4Fe-4S]$^{2+}$/Fe^{2+}−CO		1389	*20*
SiR-HP [4Fe-4S]$^{+}$/Fe^{2+}−CO		1391	*20*
NiR [4Fe-4S]$^{2+}$/Fe^{3+}	1379		*22*, our data
NiR [4Fe-4S]$^{2+}$/Fe^{3+}−CN$^-$	1379		our data
NiR [4Fe-4S]$^{2+}$/Fe^{2+}−NO		1391	our data
NiR [4Fe-4S]$^{2+}$/Fe^{3+}−NO	1381		our data
NiR [4Fe-4S]$^{2+}$/Fe^{3+}−NO_2^-	1383		our data

The resonance Raman spectrum of the EPR-silent complex formed by the reaction of [4Fe-4S]$^{2+}$/Fe^{3+} NiR with nitrite ([4Fe-4S]$^{2+}$/Fe^{3+}−NO_2^-) is most compatible with the siroheme being in an Fe^{3+}, low-spin, six-coordinate state and is consistent with earlier magnetization data which show that the siroheme is in an $S = {}^1/_2$ spin state (*11*). If this spectrum is compared with that of [4Fe-4S]$^{2+}$/Fe^{3+} NiR, the 1464 cm^{-1} band (ν_{28}) is shifted up to 1476 cm^{-1}, consistent with the presence of low-spin siroheme in the complex. The 1383 cm^{-1} band that can be attributed to the ν_4 mode is consistent with the iron being in the Fe^{3+} oxidation state, this value being more similar to that of 1379 cm^{-1} observed for the Fe^{3+} siroheme in [4Fe-4S]$^{2+}$/Fe^{3+} NiR and in the [4Fe-4S]$^{2+}$/Fe^{3+}−CN$^-$ complex than it is to the 1391 cm^{-1} band observed for the Fe^{2+} siroheme of the [4Fe-4S]$^{2+}$/Fe^{2+}−NO complex. Although the frequencies of the bands corresponding to the ν_{37} and ν_{10} modes are compatible with a low-spin, six-coordinate Fe^{3+} siroheme, they are unusually broad (fwhm of 37 and 42 cm^{-1} vs fwhm of 14 and 15 cm^{-1}, respectively, for [4Fe-4S]$^{2+}$/Fe^{3+} NiR). Curiously, no other bands are seen to broaden. These ν_{37} and ν_{10} modes are very sensitive to the core size and ruffling (*23*) of the siroheme. Their observed broadening indicates a marked heterogeneity in the core size of the siroheme, yet the lack of broadening of other bands suggests that the overall position of the siroheme in its binding pocket is not significantly perturbed or altered by formation of a complex with nitrite. One plausible interpretation of these very localized effects is that the unidentified ligand in the EPR-silent complex binds to the siroheme Fe^{3+} in a manner that is very heterogeneous with respect to parameters such as distance, geometry, and perhaps even the chemical identity of the ligand. Another possibility is that the ligand binding causes a heterogeneous siroheme ruffling. We stress that this heterogeneity appears to be localized near the Fe^{3+} center of the siroheme core and does not extend significantly to other aspects of interactions of siroheme with its binding pocket in the protein. The observation described above is compatible with the *g* strain argument being the cause for the EPR silence of the complex, resulting from the reaction of [4Fe-4S]$^{2+}$/Fe^{3+} NiR with nitrite.

The most intriguing question about the EPR-silent complex, resulting from the reaction of [4Fe-4S]$^{2+}$/Fe^{3+} NiR with

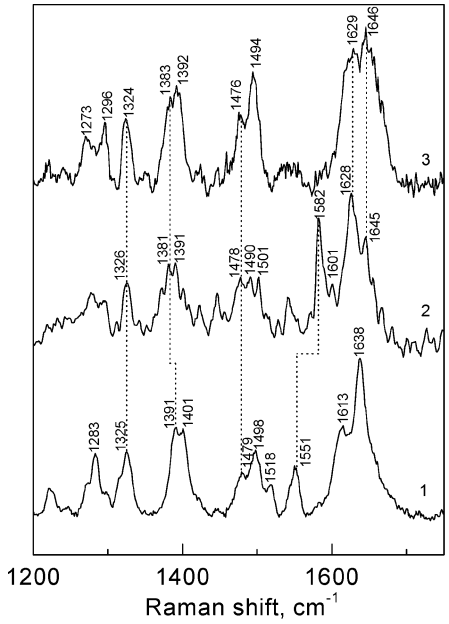

FIGURE 4: Comparison of the room-temperature resonance Raman spectrum of the nitrite adduct of oxidized $[4Fe\text{-}4S]^{2+}/Fe^{3+}$ NiR to the spectra of the complexes of nitric oxide with oxidized $[4Fe\text{-}4S]^{2+}/Fe^{3+}$ and reduced $[4Fe\text{-}4S]^{2+}/Fe^{2+}$ NiR: NiR $[4Fe\text{-}4S]^{2+}/Fe^{2+}-NO$ (same as in Figure 2), NiR $[4Fe\text{-}4S]^{2+}/Fe^{3+}-NO$ (NO-saturated water added to a degassed $[4Fe\text{-}4S]^{2+}/Fe^{3+}$ NiR sample to final concentrations of 98 μM $[4Fe\text{-}4S]^{2+}/Fe^{3+}$ NiR and 250 μM NO), and NiR $[4Fe\text{-}4S]^{2+}/Fe^{3+}-NO_2^-$ (same as in Figure 2). The exposure time for the NiR $[4Fe\text{-}4S]^{2+}/Fe^{3+}-NO$ complex was 40 s per spectrum, and the presented curve is an average of 75 spectra.

nitrite, is the identity of the sixth heme ligand. We were not able to obtain any direct evidence that the ligand is nitrite itself, as no new bands that could be attributed to nitrite vibrations were found after addition of nitrite to the enzyme in either the region near 1320 cm^{-1} or the region near 800 cm^{-1}, where one might expect to observe bands from nitrite (*38*). Varying the wavelength of laser excitation from 406.7 to 363.8, 413.1, or 441.6 nm had no effect on the absence of nitrite-attributable bands in these spectral regions. To check the possibility that the ligand in this EPR-silent complex is reduced to NO, we have compared its spectrum to the spectrum of the NO adduct of oxidized $[4Fe\text{-}4S]^{2+}/Fe^{3+}$ NiR.

Figure 4 shows the spectrum of the EPR-silent complex together with the NO complexes with oxidized ($[4Fe\text{-}4S]^{2+}/Fe^{3+}$) and reduced ($[4Fe\text{-}4S]^{2+}/Fe^{2+}$) NiR. The frequencies of spin state-sensitive bands ν_{10}, ν_{37}, and ν_{28} at 1645, 1628, and 1478 cm^{-1}, respectively, in the NiR $[4Fe\text{-}4S]^{2+}/Fe^{3+}-NO$ complex are characteristic of a low-spin siroheme. The ν_4 band is at 1381 cm^{-1}, as we would now expect for ferric siroheme in NiR. Both facts support the idea that a NO complex with oxidized $[4Fe\text{-}4S]^{2+}/Fe^{3+}$ NiR is indeed formed. The ν_{10} and ν_{37} bands in the NiR $[4Fe\text{-}4S]^{2+}/Fe^{3+}-NO$ complex exhibit exactly the same frequencies as in the EPR-silent complex, resulting from the reaction of $[4Fe\text{-}4S]^{2+}/Fe^{3+}$ NiR with nitrite. As these bands are sensitive to the nature of the ligand, this coincidence indicates the similar nature and strength of the ligand in both complexes. However, their spectra are strikingly different in the 1475–1510 cm^{-1} region, where the resonance Raman spectrum of the nitrite complex exhibits two bands while that of the NO complex shows three bands. In addition, a single band between 1520 and 1590 cm^{-1} is present in the spectra of the complexes of both $[4Fe\text{-}4S]^{2+}/Fe^{3+}$ NiR and $[4Fe\text{-}4S]^{2+}/Fe^{2+}$ NiR with NO, while this feature is absent in the spectra of all the other NiR complexes (Figure 3) and thus most likely does not arise from a siroheme vibrational mode. This band probably corresponds to the 1555 cm^{-1} band in the resonance Raman spectrum of the SiR-HP $[4Fe\text{-}4S]^{2+}/Fe^{2+}-NO$ complex, a feature that has been unambiguously assigned to NO stretch on the basis of its isotope shifts (*21*). The spectrum of the SiR-HP $[4Fe\text{-}4S]^{2+}/Fe^{3+}-NO$ complex was not observed by Han *et al*. (*21*) due to photoreduction of this state at room temperature and its photodecomposition at 77 K (*21*), and no resonance Raman spectra of a ferric isobacteriochlorin–NO complex have ever been reported. However, the NO stretching band can be expected to shift to higher frequency in the ferric heme–NO complex, in comparison to its complex with ferrous heme, due to a weaker Fe–NO bond and thus stronger N–O bond in the case of ferric heme. Thus, an assignment of the 1582 cm^{-1} band in the NiR $[4Fe\text{-}4S]^{2+}/Fe^{3+}-NO$ complex to the NO stretching seems to be reasonable. As the resonance Raman spectrum of the EPR-silent complex exhibits no band in that region, the sixth iron ligand in this complex cannot be attributed to nitric oxide.

Our data thus support the conclusion that the siroheme in the EPR-silent complex, resulting from the reaction of $[4Fe\text{-}4S]^{2+}/Fe^{3+}$ NiR with nitrite, is in the low-spin, six-coordinate Fe^{3+} state. The identity of the ligand could not be directly determined; however, it is unlikely to be nitric oxide, but seems similar to it in terms of the frequencies of the observed ν_{10} and ν_{37} modes. This fact, and the absence of any detectable intermediate during the formation of the complex from $[4Fe\text{-}4S]^{2+}/Fe^{3+}$ NiR and nitrite, strongly suggest that this ligand is the nitrite ion which is not enhanced in the resonance Raman spectrum. Finally, the relative broadening of ligand-sensitive bands ν_{10} and ν_{37} is quite consistent with the existence of a broad distribution of ligand positions and geometries and/or ruffled heme conformations, leading to a broadening of the ferric siroheme EPR signal beyond detection (*g* strain). It should be noted that the substrate binding in a variety of positions is unusual for an enzyme–substrate complex taking part in the catalysis. While the transfer of an electron from the siroheme to the ligand could be possible for a such variety of multiple bound conformations, one could expect a well-oriented substrate position to be required for efficient catalysis. It is possible that such a well-oriented position of the bound substrate is attained after the siroheme reduction (see above).

Reaction of Oxidized NiR with Hydroxylamine. It has been reported that hydroxylamine, a putative intermediate in reduction of nitrite to ammonia catalyzed by nitrite reductase, forms a 1:1 complex with NiR, with a dissociation constant of 4.2 mM (*10*). It has also been demonstrated that NH_2OH reacts with oxidized $[4Fe\text{-}4S]^{2+}/Fe^{3+}$ nitrite reductase to form another intermediate in the NiR catalytic cycle, the $[4Fe\text{-}4S]^{2+}/Fe^{2+}-NO$ complex (*4*, *18*). The absorption spectrum in the visible region during the reaction of oxidized $[4Fe\text{-}4S]^{2+}/Fe^{3+}$ NiR with excess hydroxylamine shows a single set of well-defined isosbestic points, indicating a direct conversion from one state to another (data not shown). The absorption spectrum of the NiR/NH_2OH mixture at the

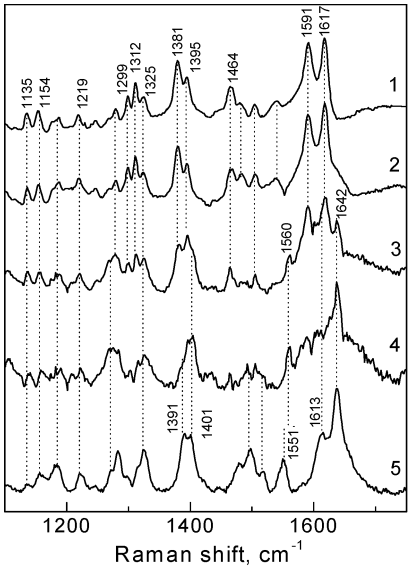

FIGURE 5: Low-temperature (15 K) resonance Raman spectra of [4Fe-4S]$^{2+}$/Fe^{3+} NiR during its reaction with hydroxylamine, obtained with Soret excitation (406.7 nm): (1) 1560 μM [4Fe-4S]$^{2+}$/Fe^{3+} NiR, (2) 940 μM [4Fe-4S]$^{2+}$/Fe^{3+} NiR and 10 mM hydroxylamine, with incubation for 2 min at room temperature, (3) sample 2, incubated for 50 min at room temperature, (4) spectrum 3 minus 0.3 $\times$ spectrum 1, and (5) NiR [4Fe-4S]$^{2+}$/Fe^{2+}−NO spectrum (same as in Figure 2). Spectra 1−3 were recorded at 15 K, and spectrum 5 was recorded at room temperature. The exposure time for spectra 1−3 was 5 s, and the presented curves are averages of 750 (1 and 2) and 2000 (3) spectra.

beginning of the incubation is identical to that of the free enzyme. The difference spectrum, taken after completion of the reaction, is in excellent agreement with the difference spectrum obtained by subtracting the spectrum of the native enzyme from the spectrum of [4Fe-4S]$^{2+}$/Fe^{3+} NiR incubated with excess hydroxylamine that was reported by Vega and Kamin (*10*). Our previous EPR study has shown that the final product of the reaction of [4Fe-4S]$^{2+}$/Fe^{3+} NiR with NH_2OH is the [4Fe-4S]$^{2+}$/Fe^{2+}−NO complex, while at the beginning of the incubation, the [4Fe-4S]$^{2+}$/Fe^{3+} NiR/NH_2-OH mixture shows only a high-spin ferric siroheme EPR signal typical of free oxidized [4Fe-4S]$^{2+}$/Fe^{3+} NiR (*18*). The absence of visible intermediates between free oxidized [4Fe-4S]$^{2+}$/Fe^{3+} NiR and the [4Fe-4S]$^{2+}$/Fe^{2+}−NO complex as determined either by EPR (*18*) or by absorption spectroscopy suggests that the NiR + NH_2OH → NiR^{-}−NO reaction includes a rate-limiting step, which occurs on the minute time scale, while all the other steps are much faster. The presence of the EPR signal characteristic of free, uncomplexed [4Fe-4S]$^{2+}$/Fe^{3+} NiR after a short incubation indicates that this limiting step is most likely the binding of hydroxylamine. We have checked this possibility by resonance Raman spectroscopy.

The results of the resonance Raman study of the reaction of oxidized [4Fe-4S]$^{2+}$/Fe^{3+} NiR with excess hydroxylamine are presented in Figure 5. For these experiments, the resonance Raman spectra of the samples, which had been frozen to stop the reaction, were measured in a cryostat in an attempt to detect possible intermediate states. The resonance Raman spectra of the enzyme at 15 K are quite similar to the room-temperature spectra, and there are only minor frequency shifts in most of the bands. The low-temperature (15 K) resonance Raman spectrum of oxidized [4Fe-4S]$^{2+}$/Fe^{3+} NiR incubated with NH_2OH for 2 min (Figure 5, curve 2) and then flash-frozen in liquid nitrogen is essentially identical to that of the free enzyme (Figure 5, curve 1). The ν_{10} and ν_{37} bands seen in the spectrum of this sample, in which [4Fe-4S]$^{2+}$/Fe^{3+} NiR and hydroxylamine were incubated together for only a short time before being frozen, are at 1617 and 1591 cm^{-1}, respectively, at exactly the same frequencies as in the spectrum of free oxidized [4Fe-4S]$^{2+}$/Fe^{3+} NiR. As the frequencies of these bands are very sensitive to the nature of the sixth siroheme iron ligand, it is unlikely that the ligand is different in the samples corresponding to spectra 1 and 2 in Figure 5. Thus, at this short incubation time (Figure 5, curve 2), the NH_2OH is most likely not yet extensively bound to the enzyme.

When the same sample is incubated for 50 min and then frozen, the resonance Raman spectrum changes dramatically (Figure 5, curve 3). The most evident differences are the appearance of a new band at 1642 cm^{-1} and a shoulder at 1401 cm^{-1}, which suggest the formation of a new species in which the siroheme is in a low-spin state. As many of the bands characteristic of free oxidized [4Fe-4S]$^{2+}$/Fe^{3+} NiR are still present in this spectrum (Figure 5, curve 3), it appears to correspond to a mixture of free oxidized [4Fe-4S]$^{2+}$/Fe^{3+} NiR with a new complex. The spectrum of the latter can be obtained by subtracting the spectrum of free oxidized [4Fe-4S]$^{2+}$/Fe^{3+} NiR (Figure 5, curve 1) from the spectrum of the mixture (Figure 5, curve 3). The result is shown as curve 4. This difference spectrum exhibits a close resemblance to the room-temperature spectrum of the [4Fe-4S]$^{2+}$/Fe^{2+}−NO complex, obtained by incubating [4Fe-4S]$^{2+}$/Fe^{3+} NiR with a large excess of hydroxylamine for long periods of time (Figure 5, curve 5). The only difference between the two spectra is that the 1551 cm^{-1} band of the room-temperature [4Fe-4S]$^{2+}$/Fe^{2+}−NO spectrum (Figure 5, curve 5), attributed to NO stretching (see above), seems to be shifted up to 1560 cm^{-1} in the calculated difference spectrum (Figure 5, curve 4). This shift, however, is most likely due to the difference in the band positions between the low-temperature and room-temperature spectra of NiR which is significant in 1510−1580 cm^{-1} region (6 cm^{-1} for the 1535 cm^{-1} band in the room-temperature spectrum of the free oxidized [4Fe-4S]$^{2+}$/Fe^{3+} enzyme), but does not exceed 1 cm^{-1} for the rest of the spectrum (results not shown).

There are no new bands in spectrum 3 that could not be attributed either to the free oxidized [4Fe-4S]$^{2+}$/Fe^{3+} NiR or to the newly formed [4Fe-4S]$^{2+}$/Fe^{2+}−NO complex. This is consistent with the absence of observable intermediates in the reaction of oxidized [4Fe-4S]$^{2+}$/Fe^{3+} NiR with hydroxylamine between the free oxidized [4Fe-4S]$^{2+}$/Fe^{3+} enzyme and the final product of this reaction, the [4Fe-4S]$^{2+}$/Fe^{2+}−NO complex, either in the UV−visible absorption spectra or in the EPR spectrum (see above). The observations that, during the first minutes of incubation of [4Fe-4S]$^{2+}$/Fe^{3+} NiR with NH_2OH, the sample has exactly the same resonance Raman, absorption, and EPR spectra as the free oxidized [4Fe-4S]$^{2+}$/Fe^{3+} enzyme show that hydroxylamine is probably not yet bound to the siroheme. These observations strongly support the hypothesis that the rate-limiting step in the reaction between oxidized [4Fe-4S]$^{2+}$/Fe^{3+} NiR and NH_2-OH is the binding itself.

CONCLUSIONS

We have studied the reaction of oxidized $[4Fe\text{-}4S]^{2+}/Fe^{3+}$ nitrite reductase with its natural substrate, nitrite, and a purported intermediate in the enzyme catalytic cycle, hydroxylamine. Hydroxylamine reacts with oxidized $[4Fe\text{-}4S]^{2+}/Fe^{3+}$ NiR in a binding-limited reaction resulting in hydroxylamine oxidation at the active site of the enzyme and formation of a nitric oxide complex with reduced siroheme. As the reaction is binding-limited, the complex between the $[4Fe\text{-}4S]^{2+}/Fe^{3+}$ NiR and hydroxylamine could not be detected, and its characteristics are still unknown.

Nitrite is shown to bind to oxidized $[4Fe\text{-}4S]^{2+}/Fe^{3+}$ NiR to form an unexpectedly EPR-silent complex, in which the NiR siroheme is most likely oxidized and low-spin. The sixth ligand of the siroheme in this complex is shown not to be nitric oxide and is most probably NO_2^-. Moreover, as seen from the unusual broadening of two ligand-sensitive Raman bands, this ligand probably binds in a heterogeneous manner, resulting in a broad distribution of different ligand interactions with the heme iron, and/or heme ruffling conformations.

ACKNOWLEDGMENT

We thank Dr. Miruna Roman for her help with the stopped-flow experiments and Dr. Jérôme Santolini for his suggestions about the method for formation of the NiR $[4Fe\text{-}4S]^{2+}/Fe^{3+}$−NO complex. We are grateful to Dr. Bernard Lagoutte for biochemistry help.

REFERENCES

1. Knaff, D. B., and Hirasawa, M. (1991) Ferredoxin-dependent chloroplast enzymes, *Biochim. Biophys. Acta 1056*, 93−125.
2. Murphy, M. J., Siegel, L. W., Tove, S. R., and Kamin, H. (1974) Siroheme: a new prosthetic group participating in six-electron reduction reactions catalyzed by both sulfite and nitrite reductases, *Proc. Natl. Acad. Sci. U.S.A. 71*, 612−616.
3. Aparicio, P. J., Knaff, D. B., and Malkin, R. (1975) The role of an iron−sulfur center and siroheme in spinach nitrite reductase, *Arch. Biochem. Biophys. 169*, 102−107.
4. Lancaster, J. R., Vega, J. M., Kamin, H., Orme-Johnson, N. R., Orme-Johnson, W. H., Krueger, R. J., and Siegel, L. M. (1979) Identification of the iron−sulfur center of spinach ferredoxin-nitrite reductase as a tetranuclear center, and preliminary EPR studies of mechanism, *J. Biol. Chem. 254*, 1268−1272.
5. Hirasawa, M., Tollin, G., Salamon, Z., and Knaff, D. B. (1994) Transient kinetic and oxidation−reduction studies of spinach ferredoxin:nitrite oxidoreductase, *Biochim. Biophys. Acta 1185*, 336−345.
6. Crane, B. R., Siegel, L. M., and Getzoff, E. D. (1995) Sulfite reductase structure at 1.6 Å: evolution and catalysis for reduction of inorganic anions, *Science 270*, 59−67.
7. Crane, B. R., Siegel, L. M., and Getzoff, E. D. (1997) Probing the catalytic mechanism of sulfite reductase by X-ray crystallography: structures of the *Escherichia coli* hemoprotein in complex with substrates, inhibitors, intermediates, and products, *Biochemistry 36*, 12120−12137.
8. Crane, B. R., and Getzoff, E. D. (1996) The relationship between structure and function for the sulfite reductases, *Curr. Opin. Struct. Biol. 6*, 744−756.
9. Young, L. J., and Siegel, L. M. (1988) On the reaction of ferric heme proteins with nitrite and sulfite, *Biochemistry 27*, 2790−2800.
10. Vega, J. M., and Kamin, H. (1977) Spinach nitrite reductase. Purification and properties of a siroheme-containing iron−sulfur enzyme, *J. Biol. Chem. 252*, 896−909.
11. Day, E. P., Peterson, J., Bonvoisin, J. J., Young, L. J., Wilkerson, J. O., and Siegel, L. M. (1988) Magnetization of the sulfite and nitrite complexes of oxidized sulfite and nitrite reductases: EPR silent spin $S = 1/2$ states, *Biochemistry 27*, 2126−2132.
12. Cammack, R., Hucklesby, D. P., and Hewitt, E. J. (1978) Electron-paramagnetic-resonance studies of the mechanism of leaf nitrite reductase. Signals from the iron-sulphur centre and haem under turnover conditions, *Biochem. J. 171*, 519−526.
13. Janick, P. A., Rueger, D. C., Krueger, R. J., Barber, M. J., and Siegel, L. M. (1983) Characterization of complexes between *Escherichia coli* sulfite reductase hemoprotein subunit and its substrates sulfite and nitrite, *Biochemistry 22*, 396−408.
14. Hewitt, E. J. (1975) Assimilatory nitrate-nitrite reduction, *Annu. Rev. Plant Physiol. 26*, 73−100.
15. Angove, H. C., Cole, J. A., Richardson, D. J., and Butt, J. N. (2002) Protein film voltammetry reveals distinctive fingerprints of nitrite and hydroxylamine reduction by a cytochrome C nitrite reductase, *J. Biol. Chem. 277*, 23374−23381.
16. Einsle, O., Messerschmidt, A., Stach, P., Bourenkov, G. P., Bartunik, H. D., Huber, R., and Kroneck, P. M. H. (1999) Structure of cytochrome *c* nitrite reductase, *Nature 400*, 476−480.
17. Einsle, O., Messerschmidt, A., Huber, R., Kroneck, P. M., and Neese, F. (2002) Mechanism of the six-electron reduction of nitrite to ammonia by cytochrome *c* nitrite reductase, *J. Am. Chem. Soc. 124*, 11737−11745.
18. Kuznetsova, S., Knaff, D. B., Hirasawa, M., Lagoutte, B., and Sétif, P. (2004) Mechanism of spinach chloroplast ferredoxin-dependent nitrite reductase: spectroscopic evidence for intermediate states, *Biochemistry 43*, 510−517.
19. Underwood-Lemons, T., Moura, I., and Yue, K. T. (1993) Resonance Raman study of sirohydrochlorin and siroheme in sulfite reductases from sulfate reducing bacteria, *Biochim. Biophys. Acta 1157*, 275−284.
20. Han, S., Madden, J. F., Thompson, R. G., Strauss, S. H., Siegel, L. M., and Spiro, T. G. (1989) Resonance Raman studies of *Escherichia coli* sulfite reductase hemoprotein. 1. Siroheme vibrational modes, *Biochemistry 28*, 5461−5471.
21. Han, S., Madden, J. F., Siegel, L. M., and Spiro, T. G. (1989) Resonance Raman studies of *Escherichia coli* sulfite reductase hemoprotein. 3. Bound ligand vibrational modes, *Biochemistry 28*, 5477−5485.
22. Ondrias, M. R., Carson, S. D., Hirasawa, M., and Knaff, D. B. (1985) Characterization of the siroheme active site in spinach nitrite reductase by resonance Raman spectroscopy, *Biochim. Biophys. Acta 830*, 159−163.
23. Melamed, D., Sullivan, E. P., Prendergast, K., Strauss, S. H., and Spiro, T. G. (1991) Analysis of a siroheme model compound: Core-size dependence of resonance Raman bands and the siroheme spin state in sulfite reductase, *Inorg. Chem. 30*, 1308−1319.
24. Hirasawa, M., Fukushima, K., Tamura, G., and Knaff, D. B. (1984) Immunochemical characterization of nitrite reductases from spinach leaves, spinach roots and other higher plants, *Biochim. Biophys. Acta 791*, 145−154.
25. Ida, S., and Mikami, B. (1986) Spinach ferredoxin-nitrite reductase: A purification procedure and characterization of chemical properties, *Biochim. Biophys. Acta 871*, 167−176.
26. Bellissimo, D. B., and Privalle, L. S. (1995) Expression of spinach nitrite reductase in *Escherichia coli*: site-directed mutagenesis of predicted active site amino acids, *Arch. Biochem. Biophys. 323*, 155−163.
27. Wilkerson, J. O., Janick, P. A., and Siegel, L. M. (1983) Electron paramagnetic resonance and optical spectroscopic evidence for interaction between sirheme and tetranuclear iron−sulfur center prosthetic groups in spinach ferredoxin-nitrite reductase, *Biochemistry 22*, 5048−5054.
28. Feelisch, M., Kubitzek, D., and Werrigloer, J. (1996) The oxyhemoglobin assay, in *Methods in nitric oxide research* (Feelisch, M., and Stamler, J. S., Eds.) Wiley, Chichester, U.K.
29. Wanat, A., Schneppensieper, T., Stochel, G., van Eldik, R., Bill, E., and Wieghardt, K. (2002) Kinetics, mechanism, and spectroscopy of the reversible binding of nitric oxide to aquated iron(II). An undergraduate text book reaction revisited, *Inorg. Chem. 41*, 4−10.
30. Kominami, S., Yamazaki, T., Koga, T., and Hori, H. (1999) EPR studies on the photo-induced intermediates of ferric NO complexes of rat neuronal nitric oxide synthase trapped at low temperature, *J. Biochem. 126*, 756−761.
31. Hirasawa, M., Shaw, R. W., Palmer, G., and Knaff, D. B. (1987) Prosthetic group content and ligand-binding properties of spinach nitrite reductase, *J. Biol. Chem. 262*, 12428−12433.

32. Mikami, B., and Ida, S. (1989) Spinach ferredoxin-nitrite reductase: characterization of catalytic activity and interaction of the enzyme with substrates, *J. Biochem. 105*, 47−50.
33. Krueger, R. J., and Siegel, L. M. (1982) Spinach siroheme enzymes: Isolation and characterization of ferredoxin-sulfite reductase and comparison of properties with ferredoxin-nitrite reductase, *Biochemistry 21*, 2892−2904.
34. Crane, B. R., Siegel, L. M., and Getzoff, E. D. (1997) Structures of the siroheme- and Fe_4S_4-containing active center of sulfite reductase in different states of oxidation: heme activation via reduction-gated exogenous ligand exchange, *Biochemistry 36*, 12101−12119.
35. Spiro, T. G. (1975) Resonance Raman spectroscopic studies of heme proteins, *Biochim. Biophys. Acta 416*, 169−189.
36. Spiro, T. G. (1985) Resonance Raman spectroscopy as a probe of heme protein structure and dynamics, *Adv. Protein Chem. 37*, 111−159.
37. Back, E., Burkhart, W., Moyer, M., Privalle, L., and Rothstein, S. (1988) Isolation of cDNA clones coding for spinach nitrite reductase: complete sequence and nitrate induction, *Mol. Gen. Genet. 212*, 20−26.
38. Nyquist, R. A., Putzig, C. L., and Leuters, M. A. (1997) *The handbook of infrared and Raman spectra of inorganic compounds and organic salts*, Vol. 2, Academic Press, San Diego.

BI048826R